Neurobiology of Disease 127 (2019) 502–511

Contents lists available at ScienceDirect

Neurobiology of Disease

journal homepage: www.elsevier.com/locate/ynbdi

Cardiorespiratory profiling reveals primary breathing dysfunction in *Kcna1*-null mice: Implications for sudden unexpected death in epilepsy

Hemangini Dhaibar[a], Nicole M. Gautier[a], Oleg Y. Chernyshev[b], Paari Dominic[c], Edward Glasscock[a,*]

[a] Department of Cellular Biology and Anatomy, Louisiana State University Health Sciences Center Shreveport, LA 71103, USA
[b] Department of Neurology, Division of Sleep Medicine, Louisiana State University Health Sciences Center Shreveport, LA 71103, USA
[c] Department of Internal Medicine, Section of Cardiology, Louisiana State University Health Sciences Center Shreveport, LA 71103, USA

ARTICLE INFO

Keywords:
Epilepsy
Sudden unexpected death in epilepsy (SUDEP)
Apnea
Sigh
Respiratory variability
Kv1.1
Sleep

ABSTRACT

Sudden unexpected death in epilepsy (SUDEP) is the leading cause of epilepsy-related mortality, but the relative importance of underlying cardiac and respiratory mechanisms remains unclear. To illuminate the interactions between seizures, respiration, cardiac function, and sleep that contribute to SUDEP risk, here we developed a mouse epilepsy monitoring unit (EMU) to simultaneously record video, electroencephalography (EEG), electromyography (EMG), plethysmography, and electrocardiography (ECG) in a commonly used genetic model of SUDEP, the *Kcna1* knockout (*Kcna1*$^{-/-}$) mouse. During interictal periods, *Kcna1*$^{-/-}$ mice exhibited an abnormal absence of post-sigh apneas and a 3-fold increase in respiratory variability. During spontaneous convulsive seizures, *Kcna1*$^{-/-}$ mice displayed an array of aberrant breathing patterns that always preceded cardiac abnormalities. These findings support respiratory dysfunction as a primary risk factor for susceptibility to deleterious cardiorespiratory sequelae in epilepsy and reveal a new role for *Kcna1*-encoded Kv1.1 channels in the regulation of basal respiratory physiology.

1. Introduction

People with epilepsy have up to 16-times greater risk of dying suddenly for reasons that remain unknown even after autopsy (Holst et al., 2013). These deaths are classified as sudden unexpected death in epilepsy (SUDEP) and represent the leading cause of epilepsy-related mortality, affecting about 1 in 1000 patients with epilepsy every year, and up to 1 in 169 patients with drug-resistant epilepsy (Shorvon and Tomson, 2011; Thurman et al., 2014). Because SUDEP strikes early in life, its public health burden is immense, leading to the second-most years of potential life lost among all neurological diseases (Thurman et al., 2014).

SUDEP risk factors suggest it is predominantly a seizure-related event (Devinsky et al., 2016). Early SUDEP studies in patients and animal models noted heart rate changes associated with seizures and focused on potential autonomic and cardiac causes (Bird et al., 1997; Dasheiff and Dickinson, 1986; Glasscock et al., 2010; Goldman et al., 2009; Russell, 1906). Emphasis shifted to respiratory mechanisms following the landmark retrospective study of mortality in epilepsy monitoring units (MORTEMUS), which described nine SUDEP cases with a pattern of seizures followed by terminal apnea preceding cardiac arrest, suggesting respiratory failure could be the primary seizure-related cause of death (Ryvlin et al., 2013). Identification of common mechanisms and unifying pathophysiological themes underlying SUDEP are needed to develop effective preventative measures.

A commonly utilized mouse model of SUDEP is the *Kcna1* gene knockout (*Kcna1*$^{-/-}$) mouse, which lacks Kv1.1 voltage-gated potassium channel α-subunits due to targeted gene deletion (Smart et al., 1998). *Kcna1*$^{-/-}$ mice recapitulate several important characteristics of human SUDEP, including frequent early-onset generalized tonic-clonic

Abbreviations: AP, Apnea; ATX, Ataxic breathing; AV, Atrioventricular; AVB, Atrioventricular block; BP, Bradypnea; BPM, Breaths per minute; CV, Coefficient of variation of the inter-breath intervals; ECG, Electrocardiography; EEG, Electroencephalograpy; EMG, Electromyography; EMU, Epilepsy monitoring unit; HV, Hyperventilation; KO, Knockout; M_v, Minute ventilation; NREM, Non-rapid eye movement sleep; PGES, Postictal generalized electroencephalography suppression; Pleth, Plethysmography; PVC, Premature ventricular block; REM, Rapid eye movement sleep; S, Sigh; SD, Spreading depolarization; SEB, Sinus exit block; SUDEP, Sudden unexpected death in epilepsy; TP, Tachypnea; T_v, Tidal volume; V, Ventricular; WT, Wild type

* Corresponding author.
E-mail addresses: hdhaib@lsuhsc.edu (H. Dhaibar), ngauti@lsuhsc.edu (N.M. Gautier), ochern@lsuhsc.edu (O.Y. Chernyshev), pdomi2@lsuhsc.edu (P. Dominic), aglas1@lsuhsc.edu (E. Glasscock).

https://doi.org/10.1016/j.nbd.2019.04.006
Received 14 January 2019; Received in revised form 14 March 2019; Accepted 5 April 2019
Available online 08 April 2019
0969-9961/

seizures (up to ~24/d beginning at 2–3 weeks old); seizure-related sudden death (occurring in about 75% of animals between 2 and 10 weeks old); and seizure-evoked progressive bradycardia leading to cardiac arrest (Glasscock et al., 2010; Moore et al., 2014; Smart et al., 1998). During interictal periods, *Kcna1*$^{-/-}$ mice show evidence of vagally-driven cardiac dysfunction, including increased incidence of atropine-sensitive atrioventricular conduction blocks; increased heart rate variability; and increased susceptibility to spontaneous ectopic firing of vagal axons (Glasscock et al., 2010, 2012; Mishra et al., 2017). In patients, *KCNA1* mutations also cause epilepsy, and they may increase SUDEP risk since a de novo *KCNA1* copy number variant has been identified by molecular autopsy of a human SUDEP case (Klassen et al., 2014; Zuberi et al., 1999).

Although neurocardiac phenotypes of *Kcna1*$^{-/-}$ mice have been extensively investigated, little is known about effects of spontaneous seizures on respiration or the interplay between cardiac and respiratory activity. Previous respiratory studies in *Kcna1*$^{-/-}$ mice have been limited to short-term analysis of interictal periods and inducible seizures, which may exhibit different features than spontaneous seizures, the clinical hallmark of epilepsy (Aiba and Noebels, 2015; Kline et al., 2005; Simeone et al., 2018). Therefore, the primary goal of this work was to elucidate pathomechanisms underlying SUDEP susceptibility by evaluating the cardiorespiratory profile of spontaneous seizures in *Kcna1*$^{-/-}$ mice. Specifically, this study sought to answer the question of whether respiratory or cardiac dysfunction is the most likely primary contributing factor to SUDEP risk. To address this, a rodent epilepsy monitoring unit (EMU) was developed that allows simultaneous recording of behavior (video), brain (electroencephalography; EEG), muscle (electromyography; EMG), pulmonary (plethysmography; pleth), and heart (electrocardiography; ECG) activities. However, while seeking to identify ictal respiratory dysfunction, this research also uncovered unexpected interictal breathing dysfunction in *Kcna1*$^{-/-}$ mice, suggesting Kv1.1 plays a role in regulating basal respiratory physiology.

2. Materials and methods

2.1. Animals and genotyping

Kcna1$^{-/-}$ mice (Tac:N:NIHS-BC genetic background) carry null (KO) alleles of the *Kcna1* gene generated by targeted deletion of the entire open reading frame on chromosome 6 (Smart et al., 1998). Mice were housed at 22 °C, fed ad libitum, and submitted to a 12-h light/dark cycle. For genotyping, genomic DNA was isolated by enzymatic digestion of tail clips using Direct-PCR Lysis Reagent (Viagen Biotech, Los Angeles, CA, USA). Genotypes were determined by performing PCR amplification of genomic DNA using allele specific primers. The following primer sequences were used to yield genotype-specific amplicons of ~337 bp for the wild-type (WT) allele and ~475 bp for the KO allele: a WT-specific primer (5′-GCCTCTGACAGTGACCTCAGC-3′), a KO-specific primer (5′-CCTTCTATCGCCTTCTTGACG-3′), and a common primer (5′-GCTTCAGGTTCGCCACTCCCC-3′). All experiments were performed in accordance with National Institutes of Health (NIH) guidelines with approval from the Institutional Animal Care and Use Committee of the Louisiana State University Health Sciences Center-Shreveport.

2.2. Video-plethysmography recordings

Unanesthetized WT (*Kcna1*$^{+/+}$; $n = 6$ males) and KO (*Kcna1*$^{-/-}$; $n = 5$ males, 1 female) mice (ages 27–49 d) were placed in an airtight unrestrained, whole-body plethysmograph chamber (Data Sciences International, St. Paul, MN, USA) outfitted with a digital video camera for simultaneous behavioral monitoring. While in the chamber, mice breathed normoxic (21% O_2) room air that was continually exchanged at a constant flow rate. A sensitive very low differential pressure transducer (Validyne DP45; Northridge, CA, USA) connected to the chamber converted pressure changes associated with inspiration and expiration into respiratory waveforms. Integrated temperature and humidity probes were used to monitor and compensate for changes in the ambient conditions of the chamber. For each experiment, mice were acclimatized to the chamber for 45 min, and then respiratory activity and video were simultaneously recorded for 6–8 h continuously using Ponemah acquisition software (Data Sciences International, St. Paul, MN, USA). Recording sessions were always conducted during the light phase of the day (8:00 am to 4:00 pm). The following parameters were determined using Ponemah analysis software (Data Sciences International, St. Paul, MN, USA): respiratory rate (breaths per min; BPM); tidal volume (T_v); and minute ventilation (M_v). Average respiratory parameters for each mouse were calculated by sampling 50 consecutive breaths every hour for 5 h for a total of 250 breaths. Baseline measurements were only obtained during periods when animals were stationary and at rest, as verified by video monitoring. Respiratory variability was calculated as the coefficient of variance (CV) using the formula: $CV = \sigma/\mu$, where σ is standard deviation of breath intervals and μ is mean of breath intervals.

2.3. Video-electroencephalography-electromyography-plethysmography-electrocardiography (EEG-EMG-pleth-ECG) recordings

WT and KO mice (ages 29–55 d, $n = 6$–7 per genotype including 3–4 of each sex) were anesthetized with avertin (0.02 mL/g, ip) and surgically implanted with bilateral silver wire EEG, ECG, and EMG electrodes (0.005-in. diameter) attached to a microminiature connector for recording in a tethered configuration. Avertin was prepared by mixing 250 mg 2,2,2-tribromoethanol (Sigma-Aldrich) with 155 μL 2-methyl-2-butanol (Sigma-Aldrich) dissolved in 19.75 mL double-distilled water heated to 40 °C, followed by filter-sterilization prior to use. EEG wires were inserted into the subdural space through cranial burr holes overlying parietotemporal cortex for the recording electrodes and above frontal cortex for the ground and reference electrodes, as described previously (Mishra et al., 2018). For ECG, two wires were tunneled subcutaneously on both sides of the thorax and sutured in place to record cardiac activity, as described previously (Mishra et al., 2018). For EMG, wires were directly sutured to nuchal muscle to record the muscle activity. Mice were allowed to recover from surgery for ≥48 h before recording. For recording, mice were placed in an unrestrained whole-body plethysmography chamber as described above but with a lid that was modified to accommodate wires for recording EEG-EMG-ECG in a tethered configuration. Following a 45-min acclimatization period in the chamber, video and EEG-EMG-pleth-ECG were simultaneously recorded in 6–8 h sessions during the light phase of the day (8:00 am to 4:00 pm) using Ponemah data acquisition and analysis software (Data Sciences International, St. Paul, MN, USA). Biosignals were band-pass filtered by applying 0.3-Hz high-pass and 200-Hz low-pass filters for EEG; a 3.0-Hz high-pass filter for ECG; and 10-Hz high-pass and 300-Hz low-pass filters for EMG. Sampling rates were set to 500 Hz for EEG, EMG and plethysmography and 2 kHz for ECG.

2.4. Analysis of respiratory and cardiac abnormalities

Respiratory and cardiac abnormalities were manually scored and quantified offline. The respiratory variables analyzed included hyperventilation (increased breathing rate with higher tidal volume), tachypnea (increased respiratory rate), ataxic breathing (abnormal pattern of breathing characterized by complete irregularity of breathing frequency and tidal volume), hypopnea (abnormally shallow breathing), bradypnea (abnormally slow breathing), sigh (deep augmented breath with a ≥ 25% higher amplitude and ≥ 125% higher tidal volume compared to the preceding 10 s), apnea (cessation of plethysmographic signals for ≥2 respiratory cycles, or 0.8-s, as estimated from the average respiratory rate in our studies), gasp (breaths with low inspiration-expiration ratio), and Cheyne–Stokes respiration

(progressively deeper, and sometimes faster, breathing followed by a gradual decrease that results in a temporary stop in breathing). For quantifying apneas, they were counted as a single event if they occurred within 10 s of each other. The cardiac variables analyzed included tachycardia, bradycardia, sinus exit block (SEB; transient absence of sinus node activity characterized by absence of P wave), atrioventricular (AV) block (characterized by a P wave followed by the absence of a QRS complex), premature ventricular block (PVC; wider QRS complex with altered axis and occurring prematurely), agonal QRS, ST segment depression, and QT prolongation. For ictal and peri-ictal respiratory and cardiac parameters related to rate, tachy- and brady-phenomena were defined as rate changes of at least +20% or − 20%, respectively, relative to the 20-s pre-ictal period immediately before seizure onset.

2.5. Sleep analysis

NeuroScore software (version 3.2.0; Data Sciences International, St. Paul, MN, USA) was used to determine vigilance state for every 10-s epoch by evaluating EEG/EMG frequency and amplitude characteristics, as done previously (Hajek and Buchanan, 2016): 1) Wakefulness - low amplitude, high frequency (7–13 Hz) EEG with high EMG power; 2) Non-rapid eye movement (NREM) sleep – high amplitude, low frequency (0.5–4 Hz) EEG with moderate to low EMG power; 3) Rapid eye movement (REM) sleep - moderate amplitude, moderate frequency (4.5–8 Hz) EEG with minimal EMG power except for brief bursts. For analysis in NeuroScore, the data was high-pass band filtered at 1 Hz for EEG and 10 Hz for EMG. In addition, the delta and theta powerbands for the sleep scoring protocol were set at 0.5–4 Hz and 6–9 Hz, respectively. Finally, the software threshold settings for the slow wave ratio, theta ratio, and EMG amplitude were adjusted and optimized for each recording.

2.6. Statistical analysis

Data are presented as mean ± SEM. Prism 6 for Windows (GraphPad Software Inc., La Jolla, CA, USA) was used for statistical analyses. For comparisons between genotypes, unpaired two-tailed Student's *t*-tests were used. Results were considered significant if $P < 0.05$.

3. Results

3.1. *Kcna1*$^{-/-}$ mice exhibit increased respiratory frequency and variability

Previous studies of respiration found that baseline breathing parameters were relatively normal in *Kcna1*$^{-/-}$ mice, but those analyses were limited to short-term recordings with durations of 3–5 min (Kline et al., 2005; Simeone et al., 2018). To analyze interictal breathing in greater detail, long-term (6–8 h) respiratory recordings were obtained from WT and KO mice using unrestrained whole-body plethysmography. Individual plethysmography (Pleth) respiratory waveforms appeared qualitatively similar in WT and KO mice (Fig. 1A), but respiratory rate was significantly increased by 20% in KO mice ($P = 0.0417$; Fig. 1B), suggesting abnormal mild tachypnea at rest. However, lung tidal volume and minute ventilation remained comparable between genotypes (Fig. 1C,D), as previously reported (Kline et al., 2005; Simeone et al., 2018). Baseline breathing function can also be evaluated by measuring respiratory variability using the coefficient of variation (CV) of the inter-breath intervals, which provides a measure of respiratory stability and possibly a marker of SUDEP risk (Hajek and Buchanan, 2016). The inter-breath time intervals were stable in WT mice but extremely variable in KO animals (Fig. 1E). Quantification of the variation of the inter-breath intervals revealed a significant 3-fold increase in resting baseline respiratory variability in KO mice compared to controls (Fig. 1F). Thus, long-term respiratory Pleth recordings revealed that KO mice have moderately faster and much more variable breathing than WT control mice.

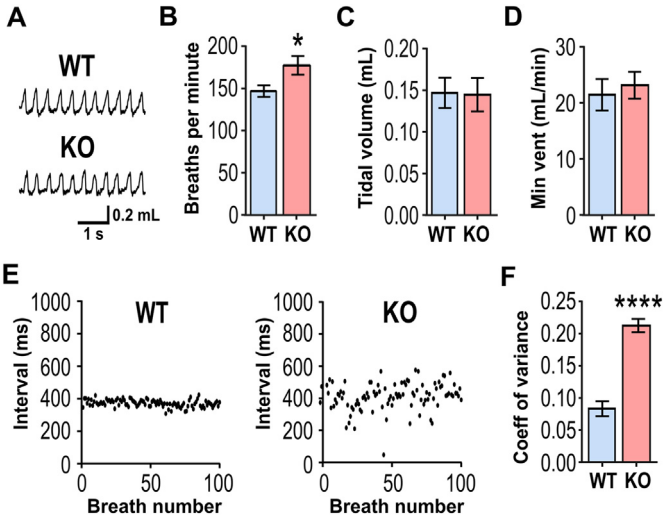

Fig. 1. *Kcna1*$^{-/-}$ mice exhibit increased respiratory rate and variability during interictal periods. (A) Representative plethysmography recordings of respiration in an unanesthetized WT and KO mice at rest. (B) Respiratory rate (breaths per min) was significantly increased in KO mice, whereas no significant differences were observed for (C) tidal volume or (D) minute ventilation (vent) between WT and KO mice. (E) Representative plots of interbreath intervals (IBI) for 100 consecutive breaths in a WT and a KO mouse while at rest. (F) Respiratory variability, measured as the IBI coefficient of variance (CV), was significantly increased by 3-fold in KO mice. $n = 6$/genotype. *, $P < 0.05$; ****, $P < 0.0001$ (unpaired two-tailed Student's *t*-test).

3.2. *Kcna1*$^{-/-}$ mice exhibit defects in post-sigh apnea generation

During respiratory recordings, three different types of apneas were observed in WT animals, consistent with previous studies in mice: 1) type 1 post-sigh apneas; 2) type 2 post-sigh apneas; and 3) spontaneous apneas (Fig. 2A) (Yamauchi et al., 2008). By definition, a type 1 post-sigh apnea is a cessation of breathing that occurs following several eupneic breaths after a sigh, whereas a type 2 post-sigh apnea occurs immediately following a sigh (Yamauchi et al., 2008). Spontaneous apneas occur without a preceding sigh (Yamauchi et al., 2008). WT animals exhibited about 16 ± 2 apneas per h, consisting of predominantly type 1 post-sigh apneas (11 ± 3 per h) and spontaneous apneas (4 ± 1 per h); type 2 post-sigh apneas were only rarely seen (1 ± 0.03 per h; Fig. 2B). In contrast, during interictal periods KO mice exhibited a nearly complete absence of all types of apneas, which were significantly reduced by 81% ($P = 0.0003$) compared to WT controls (Fig. 2B). The incidences of both type 1 post-sigh apneas ($P = 0.0011$) and spontaneous apneas ($P < 0.0001$) were significantly reduced in KO mice by about 75% (Fig. 2B). Although apnea frequency was drastically reduced in KO mice, individual apnea durations remained unchanged (Fig. 2C).

One explanation for the absence of interictal post-sigh apneas in KO mice could be a corresponding reduction in sigh occurrence since sighs trigger apneas as part of a normal reflex mechanism (Ramirez, 2014; Yamauchi et al., 2008). However, sigh frequency was similar between genotypes (Fig. 2D). Instead, the percentage of sighs that evoked an apnea was significantly ($P = 0.0012$) reduced in KO mice (12 ± 2%) compared to WT animals (47 ± 8%), suggesting Kv1.1 deficiency impairs the ability of a sigh to generate an apnea (Fig. 2E).

3.3. *Kcna1*$^{-/-}$ mice exhibit a reduction in post-sigh apnea frequency during NREM sleep

Post-sigh apneas in mice occur almost exclusively during NREM

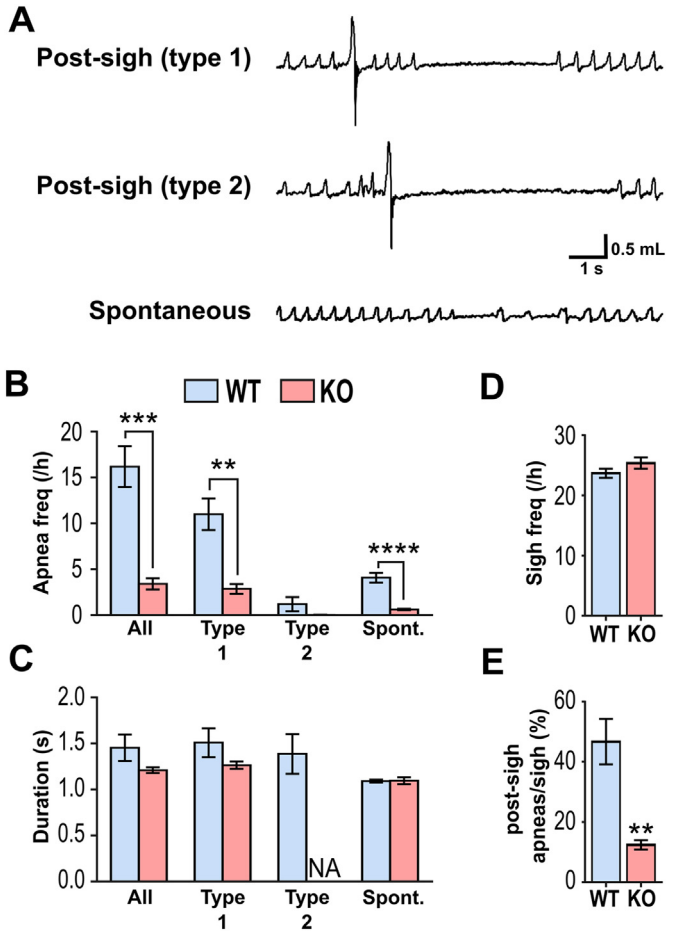

Fig. 2. *Kcna1*$^{-/-}$ mice exhibit defects in post-sigh apnea generation. (A) Representative plethysmography recordings of the different types of apneas in WT mice. (B) Quantification of apnea frequency by type, (C) apnea duration by apnea type, (D) sigh frequency per hour, and (E) percentage ratio of post-sigh apneas to total number of sighs for WT and KO mice. n = 6/genotype. **, $P < 0.01$; ***, $P < 0.001$ (unpaired two-tailed Student's t-test). NA, not available.

sleep when respiratory drive is attenuated and the metabolic drive from chemoreceptors dominates (Javaheri, 2010; Nakamura et al., 2003; Nakamura and Kuwaki, 2003). Previous studies have shown that *Kcna1*$^{-/-}$ mice spend less time in rapid eye movement sleep (REM) and non-REM sleep (NREM) and more time awake than WT animals (Roundtree et al., 2016). Thus, the reduced NREM sleep in *Kcna1*$^{-/-}$ mice could contribute to their overall reduction in interictal post-sigh apnea frequency. To test this hypothesis, a small animal epilepsy monitoring unit (EMU) was developed to simultaneously record video, EEG, EMG, Pleth, and ECG for comprehensive analyses of behavioral, brain, muscle, lung, and heart activities, respectively.

Analysis of vigilance state from the EEG and EMG signals revealed severe sleep abnormalities in *Kcna1*$^{-/-}$ mice, including drastic reductions in NREM sleep time (−42 ± 5%; $P < 0.0001$) and increased wakefulness (+50 ± 5%; $P < 0.0001$), similar to previous reports (Roundtree et al., 2016) (Fig. 3A,B). To determine whether the reduction in post-sigh apneas in KO mice was due to a lack of NREM sleep, the frequency of post-sigh apneas was calculated for each vigilance state. NREM-associated post-sigh apneas (type 1 and 2) occurred frequently in WT mice (15 ± 3 per h) as expected, but only rarely in KO mice (1 ± 1 per h; $P = 0.0022$; Fig. 3C). In addition, the percentage of sighs that evoked an apnea during NREM sleep was significantly ($P = 0.0008$) reduced in KO mice (7 ± 3%) compared to WT animals (62 ± 10%; Fig. 3D). Thus, the lack of NREM sleep time in KO mice does not appear to solely explain the drastic reduction in post-sigh apnea frequency since sighs still fail to evoke apneas in KO mice even when they are in NREM sleep.

3.4. Seizures evoke respiratory abnormalities in *Kcna1*$^{-/-}$ mice

Video-Pleth recordings were examined to determine whether KO mice exhibit respiratory abnormalities during spontaneous seizures, which were manually identified from video recordings by their characteristic convulsive behaviors, as done previously (Gautier and Glasscock, 2015). Video analyses revealed that during the plethysmography recording sessions, KO mice experienced numerous behavioral seizures of varying severity. We categorized these seizures according to the Racine scale: Stage 2 (mouth and facial movement with head nodding); Stage 3 (forelimb clonus); Stage 4 (rearing with forelimb clonus); and Stage 5 (rearing and falling with forelimb clonus). The onset of behavioral seizure activity was always associated with hyperventilatory breathing (Fig. 4). Less severe seizures (Stages 1–2) usually exhibited hyperventilation and tachypnea (Fig. 4A). In contrast, more severe seizures (Stages 3–5) manifested more adverse respiratory abnormalities including patterns of hyperventilation with tachypnea transitioning to marked ataxic or apneic breathing (Fig. 4B,C). Thus, *Kcna1*$^{-/-}$ mice exhibit ictal respiratory abnormalities that tend to increase in severity as seizure severity increases.

3.5. Seizure-evoked respiratory dysfunction precedes cardiac abnormalities in *Kcna1*$^{-/-}$ mice

Since ECG and EEG were not monitored in our initial breathing studies (Fig. 4), the interplay between cardiac and respiratory activities could not be assessed and precisely correlated with seizure epochs, which are more accurately delineated electrographically. Therefore, to identify patterns of seizure-related cardiorespiratory dysfunction that may contribute to SUDEP risk and their temporal relationship, *Kcna1*$^{-/-}$ mice were recorded using simultaneous EEG-EMG-Pleth-ECG. A total of 73 seizures were captured in 7 *Kcna1*$^{-/-}$ mice, including 29 mild (stages 1–2) and 44 severe (stages 3–5) seizures, and the incidence of ictal and post-ictal respiratory and cardiac abnormalities catalogued and quantified (Fig. 5).

During seizures, the incidence and severity of respiratory abnormalities was higher in more severe seizures, as observed in the video-EEG-EMG-Pleth-ECG recordings. The most common respiratory abnormalities observed were hyperventilation and tachypnea, occurring in > 50% of mild seizures and > 95% of severe seizures. When hyperventilation occurred, it always coincided exactly with electrographic seizure onset (Figs. 6–8), as predicted from the video-Pleth recordings (Fig. 4). Ataxic breathing, a potentially harmful respiratory pattern, occurred in 66% of severe seizures, but only in 17% of mild seizures. Other deleterious breathing patterns, including hypopnea, bradypnea, and apnea, only occurred during severe seizures and only about 9–25% of the time.

Ictal cardiac abnormalities were also present. However, they were more likely to occur during severe seizures, and their overall prevalence was much lower than respiratory abnormalities (Fig. 5C). The most common ECG abnormalities observed were tachycardia, bradycardia, sinus exit blocks, premature ventricular contractions (PVC), and atrioventricular (AV) conduction blocks, but their incidence was still relatively low, occurring in 9–23% of severe seizures. During the postictal period, the onset of cardiorespiratory abnormalities was also observed but with a much lower incidence than during seizures (Fig. 5D).

To determine whether respiratory or cardiac dysfunction is the primary defect leading to SUDEP susceptibility in *Kcna1*$^{-/-}$ mice, the temporal sequence of ictal cardiorespiratory abnormalities was analyzed. Some seizures exhibited respiratory abnormalities in the absence of obvious cardiac irregularities. For example, a Cheyne-Stokes pattern of respiration, characterized by cycles of progressively deeper breathing

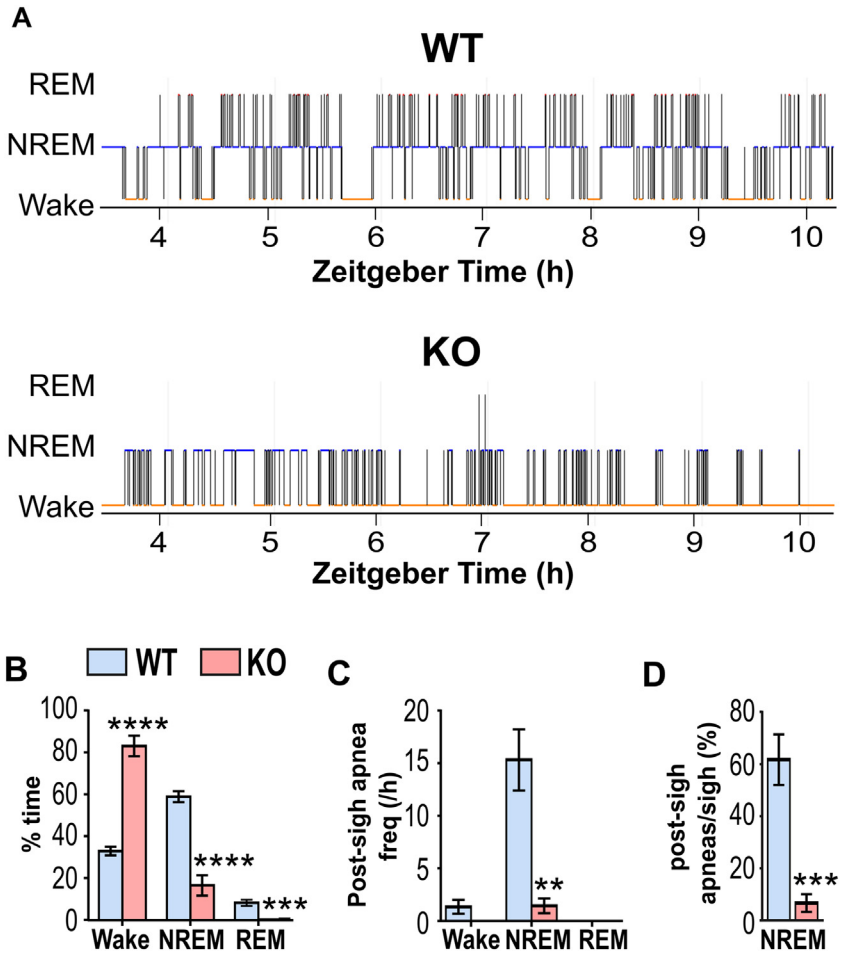

Fig. 3. *Kcna1*$^{-/-}$ mice exhibit reduced post-sigh apnea frequency during NREM sleep. (A) Representative hypnograms from unanesthesized WT and KO mice during a 6-h recording session, demonstrating reduced sleep in KO mice. (B) Quantification of percentage time spent per hour in each vigilance state for WT and KO mice reveals decreased NREM and REM sleep in KO with significantly increased wakefulness. (C) Post-sigh apnea frequency and (D) post-sigh apnea/sigh percentage were significantly reduced during NREM sleep, the predominant vigilance state for the occurrence of post-sigh apneas. n = 6/genotype. *, $P < 0.05$; **, $P < 0.01$; ****, $P < 0.001$ (unpaired two-tailed Student's t-test). NREM, non-rapid eye-movement sleep; REM, rapid eye-movement sleep.

followed by a gradual decrease that results in a brief apnea, was observed in one seizure without any obvious cardiac abnormalities or heart rate changes (Fig. 6). However, when cardiac dysfunction was present during a seizure, it was always preceded by respiratory dysfunction, usually ataxic breathing (Figs. 7, 8). Although no SUDEP events occurred during our recordings, one near SUDEP event was captured that illustrates an extreme example of respiratory-mediated ictal cardiac dysfunction (Fig. 8). In this case, a 42-s stage 5 seizure evoked a 14-s apnea followed by postictal generalized EEG suppression (PGES) and myriad ECG abnormalities such as bradycardia, premature ventricular block (PVC), sinus exit blocks (SEB), tachycardia, AV nodal block, SEB with ventricular escape beat, agonal QRS, AV block with ventricular escape beat, ST depression, and QT prolongation (Fig. 8A,C). Agonal QRS and ST depression are often indicative of hypoxia or myocardial damage. These findings support the hypothesis that the primary driver of seizure-related cardiac dysfunction in *Kcna1*$^{-/-}$ mice is aberrant respiration occurring during the seizure.

4. Discussion

This is the first study to describe the cardiorespiratory profile of spontaneous seizures in the *Kcna1*$^{-/-}$ mouse, one of the most commonly used models for investigation of SUDEP pathomechanisms. Previous studies in this model have focused on cardiac and autonomic mechanisms with ictal respiratory data limited to induced seizures, which do not meet the clinical criteria for epilepsy. Comprehensive monitoring in our rodent EMU revealed an array of breathing irregularities occurring during spontaneous seizures. These respiratory abnormalities became more severe as behavioral seizure severity increased (Fig. 4). In addition, simultaneous ECG recordings revealed that cardiac dysfunction was always closely preceded by respiratory dysfunction (Figs. 7,8), suggesting the possibility that respiratory factors trigger abnormal cardiac activity. This work also uncovered a unique effect of Kv1.1 deficiency on basal respiration: a nearly complete absence of interictal apneas (Fig. 2B). Therefore, in addition to detailing cardiorespiratory patterns underlying SUDEP susceptibility, these findings also suggest an important requirement for Kv1.1 subunits in maintaining normal respiratory physiology.

A major barrier to understanding and preventing SUDEP has been a lack of consensus on whether cardiac or respiratory dysfunction is the primary initiating factor leading to death. Cardiac events have been frequently reported associated with seizures, but these could be secondary to breathing dysfunction since concurrent respiratory monitoring has usually not been available (Bird et al., 1997; Dasheiff and Dickinson, 1986; Glasscock et al., 2010; Goldman et al., 2009; Russell, 1906). Here, we developed a rodent EMU to overcome that limitation. Recordings revealed that respiratory abnormalities in *Kcna1*$^{-/-}$ mice were much more common during seizures than cardiac dysfunction (Fig. 5C). A reliable marker of electrographic seizure onset in *Kcna1*$^{-/-}$ animals was hyperventilation and tachypnea, which almost always occurred simultaneously with the beginning of seizure activity (Fig. 6–8). Importantly, ictal breathing difficulties always immediately preceded cardiac abnormalities in *Kcna1*$^{-/-}$ mice (Fig. 7C, 8C).

Since no SUDEP events were captured during our recordings, it remains unknown if or how the cardiorespiratory patterns of fatal seizures differ from nonfatal ones. However, we did observe a 42-s nonfatal seizure that we consider a near-SUDEP event since it involved an exceptionally prolonged 14-s apnea that began near the end of the seizure and continued into the postictal period (Fig. 8). This breathing cessation led to cardiac abnormalities indicative of hypoxia, including

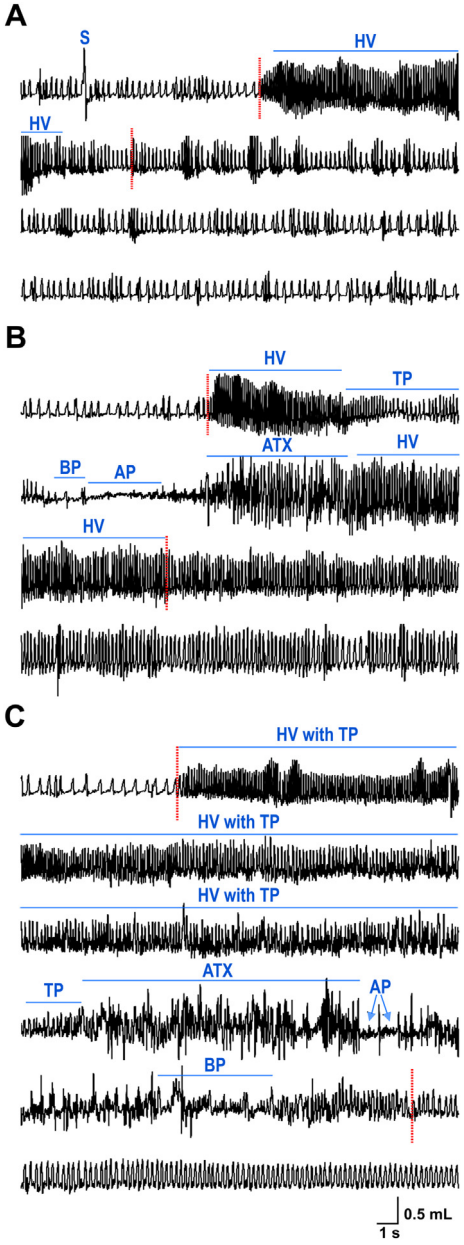

Fig. 4. Seizures evoke respiratory abnormalities in *Kcna1*$^{-/-}$ mice. Video-plethysmography recordings of (A) stage 2, (B) stage 3, and (C) stage 5 behavioral seizures according to the Racine scale: stage 2 (head nodding); stage 3 (forelimb clonus); and stage 5 (rearing and falling with forelimb clonus). Stage 5 seizures typically exhibited deleterious respiratory abnormalities characterized by patterns of hyperventilation with tachypnea transitioning to prolonged ataxic breathing with or without apnea. Onset and termination of spontaneous behavioral seizures are denoted by dotted red lines. Various types of respiratory abnormalities are labeled with lines to indicate their corresponding duration. S, sigh; HV, hyperventilation; TP, tachypnea; BP, bradypnea; AP, apnea; ATX, ataxic breathing.

ST depression and agonal QRS complexes, before normal cardiorespiratory rhythms resumed. Bradycardia and ST-segment abnormalities have also been observed in rats due to obstructive apnea caused by laryngospasm during kainic acid-induced seizures (Nakase et al., 2016). Whether the ictal apneas in our animals were central or obstructive cannot be definitively ascertained since intercostal EMG electrodes were not present.

In a study of intractable epilepsy patients, central apnea and O_2 desaturation occurred when seizures spread to the amygdala or upon amygdala stimulation, indicative of functional connectivity between the amygdala and medullary respiratory networks (Dlouhy et al., 2015). In *Kcna1*$^{-/-}$ mice, spontaneous seizures also activate the amygdala which could contribute to the manifestation of ictal breathing abnormalities (Gautier and Glasscock, 2015). A limitation of our experiments was that blood gases were not measured so changes in O_2, CO_2, or pH can only be inferred. However, pulse oximetry studies in *Kcna1*$^{-/-}$ mice show they experience frequent hypoxia with O_2 saturation levels < 90% (Simeone et al., 2018). A recent study of SUDEP-prone *Scn1a*$^{R1407X/+}$ Dravet syndrome mice is the only other study to date that has employed simultaneous monitoring of cardiac and respiratory activity with EEG to identify patterns associated with spontaneous seizures (Kim et al., 2018). Although seizures in *Scn1a*$^{R1407X/+}$ mice did not consistently evoke increases in respiratory rate at ictal onset like *Kcna1*$^{-/-}$ seizures, they did exhibit ictal apnea or respiratory depression prior to bradycardia or terminal asystole (Kim et al., 2018). Taken together, findings in *Kcna1*$^{-/-}$ and *Scn1a*$^{R1407X/+}$ mice point to the importance of respiratory mechanisms as primary initiating events leading to deleterious cardiorespiratory dysfunction underlying SUDEP risk.

The peri-ictal cardiorespiratory patterns in mouse SUDEP models exhibit both similarities and differences with those identified in SUDEP patients, providing an opportunity to identify possible unifying pathophysiological themes. In the MORTEMUS study, all SUDEP events exhibited a generalized tonic-clonic seizure followed by postictal increases in respiratory and heart rates, which gave way to a lethal combination of central apnea, bradycardia, and asystole coincident with postictal generalized EEG suppression (Ryvlin et al., 2013). In MORTEMUS patients, terminal apnea always preceded cardiac arrest suggesting the primacy of respiratory mechanisms and resembling findings in *Kcna1*$^{-/-}$ and *Scn1a*$^{R1407X/+}$ mice (Kim et al., 2018; Ryvlin et al., 2013). However, the mouse models show terminal or near fatal apnea beginning during the seizure rather than postictally as in monitored SUDEP patients.

The pattern of lethal cardiorespiratory failure preceded by respiratory depression is also present in anesthetized *Kcna1*$^{-/-}$ mice with long-duration seizures induced by topical cortical application of the potassium channel blocker 4-aminopyridine (4-AP) (Aiba and Noebels, 2015). In these animals, 4-AP-induced seizures trigger respiratory depression that begins during the ictal period and gives way to coincident postictal EEG suppression and brainstem spreading depolarization (SD) that culminates in eventual fatal cardiorespiratory arrest (Aiba and Noebels, 2015). In contrast, 4-AP-induced seizures in WT mice cause only minimal cardiorespiratory effects and fail to evoke SD and death (Aiba and Noebels, 2015). It is unlikely that the cardiorespiratory dysfunction in our recordings was caused by brainstem SD. First, brainstem SD was always fatal in *Kcna1*$^{-/-}$ mice with 4-AP-induced seizures, whereas the seizures in this study were nonfatal. Second, ictal apnea preceded SD-related arrhythmia onset in the 4-AP-induced *Kcna1*$^{-/-}$ seizure model with a latency on the order of tens of seconds to minutes, much longer than the hundreds of milliseconds to seconds latencies in this study. The shorter latencies in our study suggest the involvement of cardiorespiratory coupling reflex mechanisms rather than SD. Third, brainstem SD should exhibit a very long recovery time (Lauritzen et al., 2011) leading to prolonged cardiorespiratory depression, whereas in our animals, cardiorespiratory dysfunction was rapidly reversible (< 1 min).

One issue that remains to be resolved is whether fatal spontaneous seizures in *Kcna1*$^{-/-}$ mice exhibit the same pattern of lethal dysfunction as 4-AP-induced seizures (i.e., ictal apnea followed by postictal SD and cardiorespiratory arrest). In unpublished EEG-ECG recordings without plethysmography, we have recently captured two spontaneous SUDEP events in *Kcna1*$^{-/-}$ mice. In both cases, death was precipitated by fatal seizures that were relatively short (40 s) with running and bouncing behaviors (stage 5) and culminating in tonic extension and death. In both animals, bradycardia became apparent at 17–20 s after

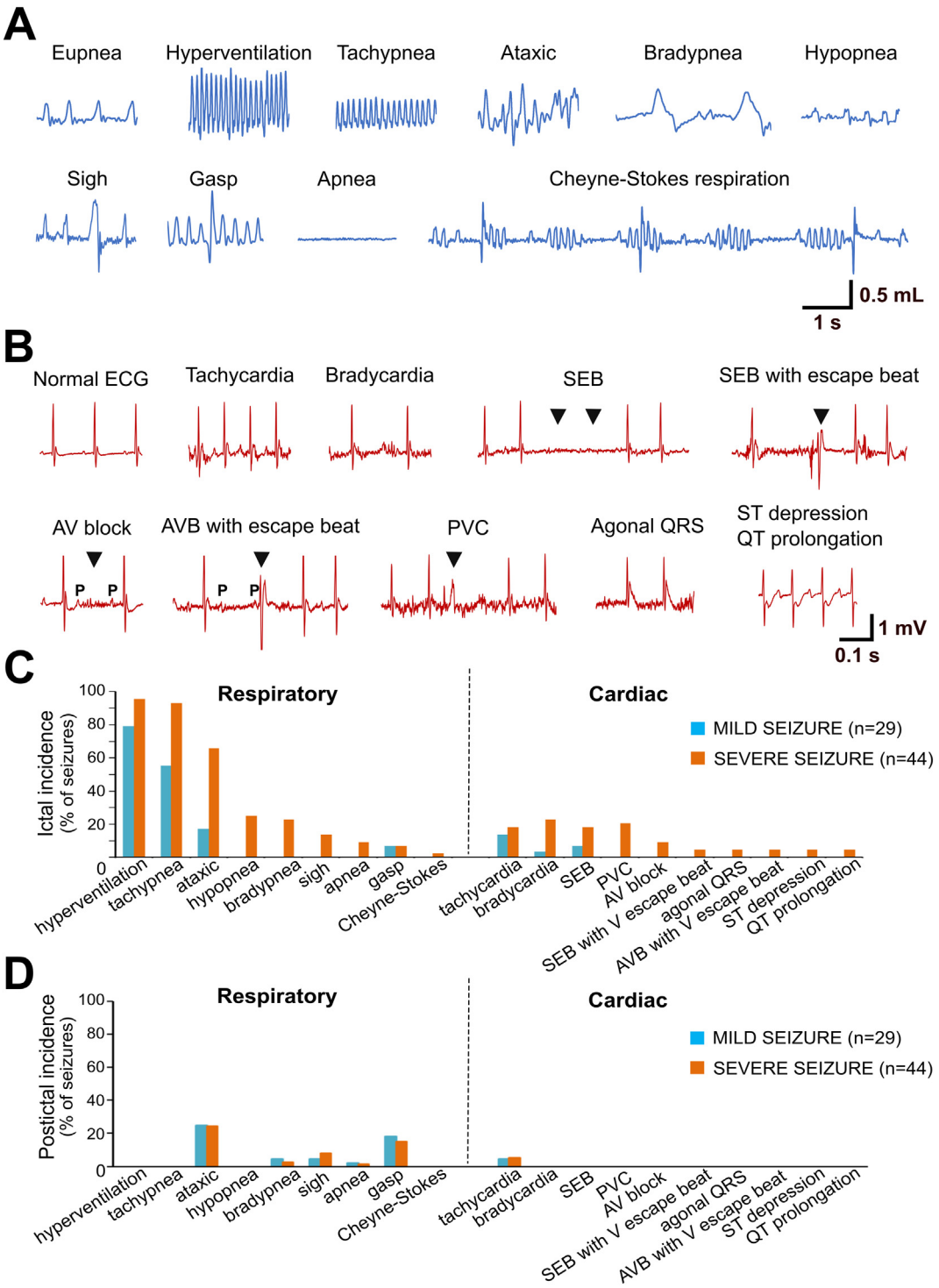

Fig. 5. *Kcna1*$^{-/-}$ mice exhibit a higher incidence of respiratory abnormalities during seizures than cardiac abnormalities. (A) Plethysmography and (B) electrocardiography (ECG) traces from KO mice showing examples of various ictal respiratory and cardiac abnormalities, respectively. Quantification of the incidence of (C) ictal and (D) postictal respiratory and cardiac abnormalities associated with mild (stage 1–2; $n = 29$) and severe (stage 3–5; $n = 44$) seizures recorded in 7 KO mice (3 male and 4 female). The postictal period was defined as the 20 s immediately after cessation of seizure. AV, atrioventricular; AVB, atrioventricular block; ECG, electrocardiogram; P, P wave; PVC, premature ventricular contraction; SEB, sinus exit block; V, ventricular.

electrographic seizure onset and about 2–3 s before the initiation of running/bouncing behaviors. Following the seizures, postictal EEG suppression was present, as well as profound bradycardia of 120–240 bpm including agonal QRS complexes indicative of severe hypoxia. Whether seizures can trigger lethal SD on such a short timescale remains to be seen since studies of fatal induced or spontaneous seizures in SUDEP mouse models show brainstem SD developing over ≥2 min during prolonged seizures of ≥3 min (Aiba and Noebels, 2015; Loonen et al., 2019).

In addition to ictal breathing phenomena, our findings reveal an important role for Kv1.1 subunits in maintaining normal basal respiratory physiology. Whereas numerous studies have identified gene mutations that increase apnea frequency (Durand et al., 2005; Marcouiller et al., 2014; Nakamura et al., 2007; Real et al., 2007;

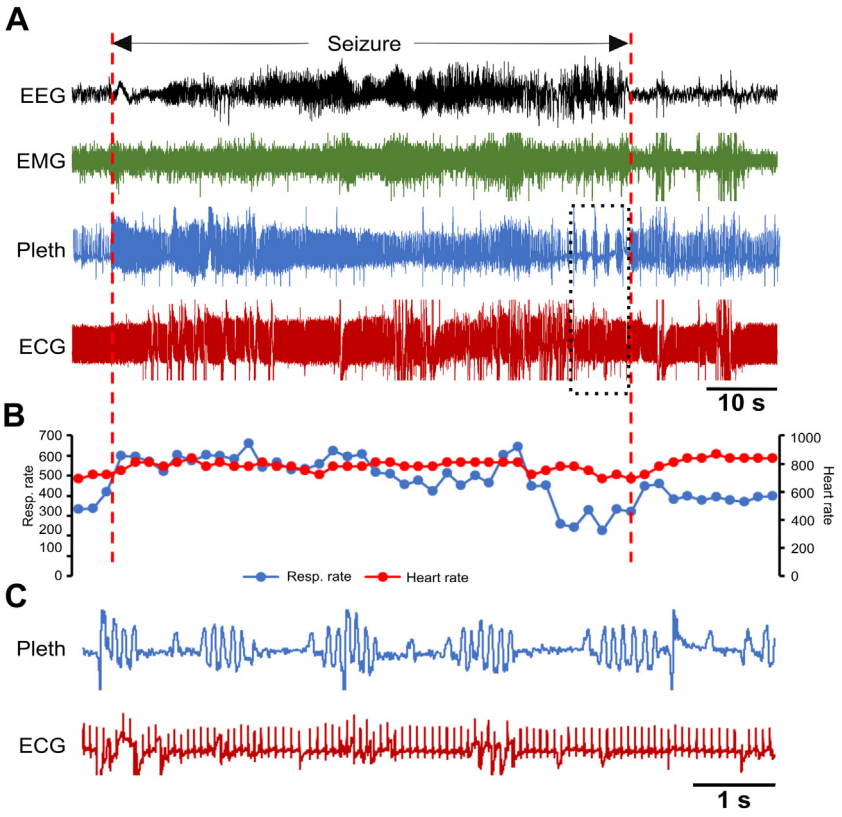

Fig. 6. Spontaneous seizure in a *Kcna1*$^{-/-}$ mouse with Cheyne-Stokes respiration and no effect on heart rate. (A) Recording of simultaneous EEG-EMG-Pleth-ECG activity during a spontaneous stage 3 seizure in a 39-day old *Kcna1*$^{-/-}$ mouse. Onset and termination of the seizure are indicated by dotted red lines. (B) Respiratory and heart rates (per min) corresponding to the recording in (A). Each dot in the plot represents the 2-s mean value. (C) Expanded traces of plethysmography and ECG for the time indicated by the boxed area showing Cheyne-Stokes respiration with no effect on the heart rate. Some movement artifacts are present in the ECG signals; therefore, scoring of heartbeats was done manually as needed. ECG, electrocardiography; EEG, electroencephalography; EMG, electromyography; Pleth, plethysmography.

Stettner et al., 2007), *Kcna1* deletion represents the first mutation to abolish apneas (Fig. 2B). Sighs trigger respiratory pauses or apneas as a normal physiological reflex response by: 1) increasing blood oxygenation, which reduces chemoreceptor-mediated respiratory drive; and/or 2) activating pulmonary stretch receptors, which increase mechanoreceptor-mediated breathing inhibition (Hering-Breuer reflex)

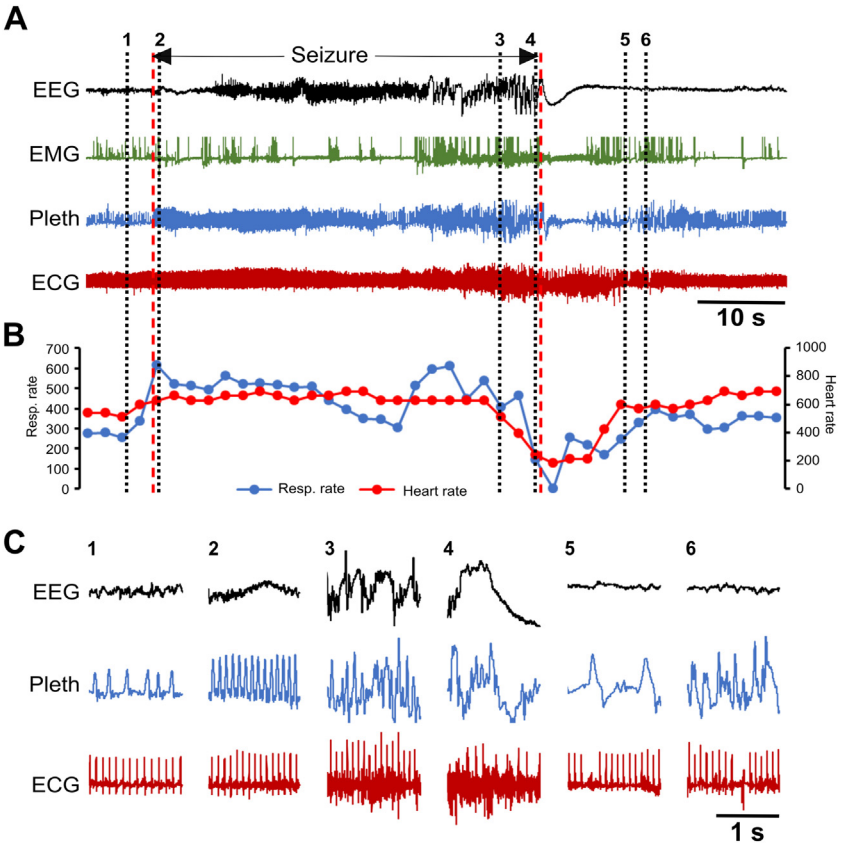

Fig. 7. Spontaneous seizure in a *Kcna1*$^{-/-}$ mouse with respiratory dysfunction preceding cardiac abnormalities. (A) Recording of simultaneous EEG-EMG-Pleth-ECG activity during a spontaneous stage 5 seizure in a 35-day old *Kcna1*$^{-/-}$ mouse. Onset and termination of the seizure are indicated by dotted red lines. (B) Respiratory and heart rates (per min) corresponding to the recording in (A). Each dot in the plot represents the 2-s mean value. (C) Expanded traces of EEG, Pleth, and ECG at the times indicated by the black dotted lines numbered 1 to 6 in (A). The numbers mark the following events: 1, pre-ictal phase; 2, hyperventilation with unchanged heart rate shortly after the onset of the seizure; 3, ictal ataxic breathing with unchanged heart rate; 4, ataxic breathing with significant bradycardia shortly before seizure termination; 5, post-ictal EEG suppression with bradypnea and a sinus exit block; 6, post-ictal ataxic breathing with a sinus exit block followed by a ventricular escape beat. Between numbers 4 and 5, a 4-s apnea occurs at the beginning of the post-ictal period. Some movement artifacts are present in the plethysmography and ECG signals; therefore, scoring of breaths and heartbeats was done manually as needed. The high frequency ECG signal noise during portions of the seizure likely reflects skeletal muscle activity. ECG, electrocardiography; EEG, electroencephalography; EMG, electromyography; Pleth, plethysmography.

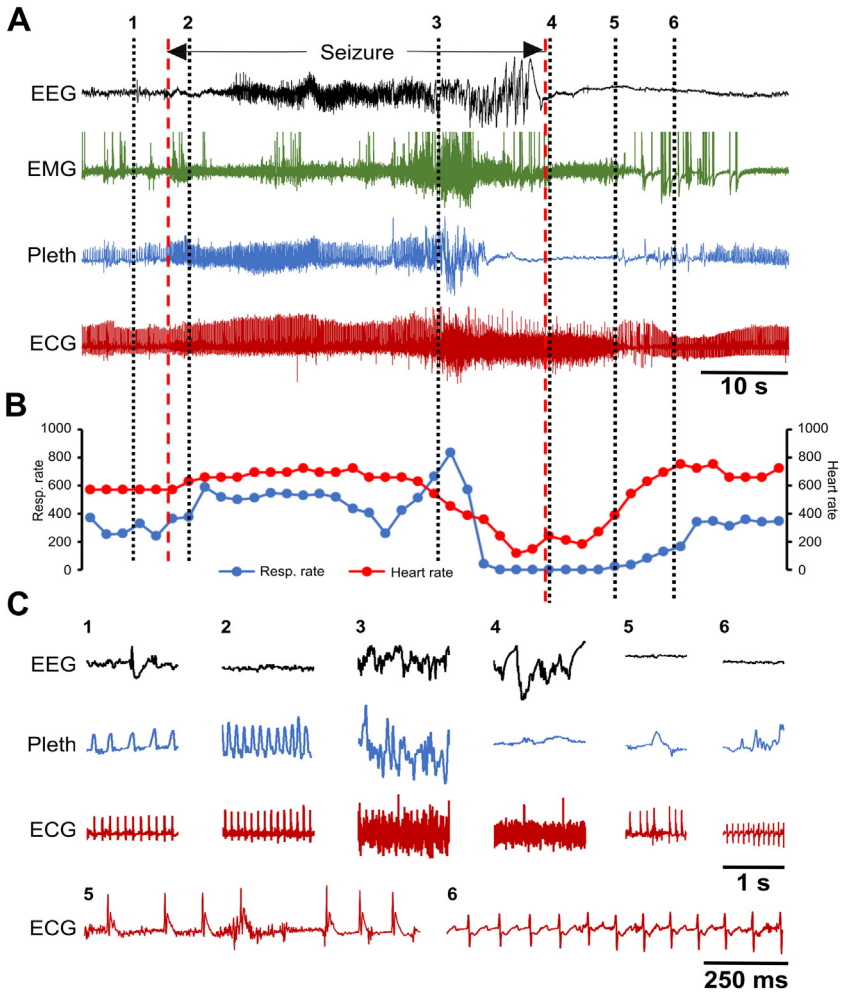

Fig. 8. Spontaneous seizure in a *Kcna1*$^{-/-}$ mouse with a prolonged 14-s apnea followed by myriad ECG abnormalities representing a possible near SUDEP event. (A) Recording of simultaneous EEG-EMG-Pleth-ECG activity during a spontaneous stage 5 seizure in a 35-day old *Kcna1*$^{-/-}$ mouse. Onset and termination of the seizure are indicated by dotted red lines. (B) Respiratory and heart rates (per min) corresponding to the recording in (A). Each dot in the plot represents the 2-s mean value. (C) Expanded traces of EEG, Pleth, and ECG at the times indicated by the black dotted lines numbered 1 to 6 in (A). The numbers mark the following events: 1, pre-ictal phase; 2, hyperventilation with unchanged heart rate shortly after the onset of the seizure; 3, ictal ataxic breathing with unchanged heart rate; 4, apnea with significant bradycardia shortly after seizure termination; 5, post-ictal EEG suppression with bradypnea and agonal QRS (ECG shown expanded below); 6, post-ictal EEG suppression with hypopnea and ECG exhibiting ST depression and QT prolongation (ECG shown expanded below). ECG, electrocardiography; EEG, electroencephalography; EMG, electromyography; Pleth, plethysmography.

(Nakamura and Kuwaki, 2003; Yamauchi et al., 2008). In mice, postsigh apneas mostly occur during NREM sleep (Nakamura et al., 2003; Nakamura and Kuwaki, 2003). However, even after accounting for NREM sleep deficits, *Kcna1*$^{-/-}$ mice still exhibited profound reductions in postsigh apnea frequency (Fig. 3C,D). Furthermore, sigh frequency was not significantly different in *Kcna1*$^{-/-}$ mice (Fig. 2D), suggesting that the defect lies in apnea generation, most notably after a sigh. One explanation for the absence of apneas could be increased peripheral chemosensory activity leading to aberrant carotid body firing following sighs, which inhibits apneas (Sheikhbahaei et al., 2017). *Kcna1* deletion increases the excitability of the afferent chemosensory pathway at the levels of the carotid bodies and the nucleus of the solitary tract which enhances respiration in response to hypoxia (Kline et al., 2005). Another explanation for the lack of apneas in *Kcna1*$^{-/-}$ mice could be altered excitability of the brainstem respiratory nuclei, such as the pre-Bötzinger complex, that control respiratory rhythms and regulate sigh-apnea coupling (Anderson and Ramirez, 2017). Interestingly, a reduction in post-sigh apneas has been observed in infants who later succumbed to sudden infant death syndrome (SIDS), possibly due to alterations in the chemoreceptor pathway (Kahn et al., 1988).

In addition to apneas, *Kcna1*$^{-/-}$ mice exhibited basal respiratory alterations manifested as increases in interictal respiratory rate and variability (Fig. 1B,E,F). Although we do not know the mechanism underlying the increased respiratory variability in *Kcna1*$^{-/-}$ mice, it may represent a marker of elevated SUDEP risk. Previously, increased respiratory variability has been linked to increased risk of death in mice following seizures induced by maximal electroshock (Hajek and Buchanan, 2016). This respiratory rhythm instability may cause vulnerability to cardiorespiratory failure triggered by a seizure, which further destabilizes the system (Hajek and Buchanan, 2016).

5. Conclusions

This study profiles patterns of cardiorespiratory activity associated with increased SUDEP risk using *Kcna1*$^{-/-}$ mice as a model. These findings emphasize the importance of respiratory mechanisms as potential initiating factors triggering deleterious cardiorespiratory dysfunction. Dissecting the relative importance of cardiac and respiratory abnormalities in SUDEP causation is imperative for identifying appropriate preventative measures, whether they should be targeted at the heart or breathing. Complicating this endeavor is genetic pleiotropy, whereby most candidate genes for SUDEP can exert dual brain-heart arrhythmogenic effects due to expression in both brain and heart tissues (Glasscock, 2014). For example, in addition to the nervous system, Kv1.1 subunits are also expressed in cardiomyocytes where their deficiency impairs heart function intrinsically (Glasscock et al., 2015; Si et al., 2018). Therefore, compromised heart function could further exacerbate the likelihood of breathing dysfunction triggering deleterious cardiac arrhythmias. In summary, this work illuminates the crossroads between respiratory and cardiac mechanisms in epilepsy, providing evidence for primary breathing dysfunction as an important risk factor for increased SUDEP susceptibility.

Funding

This work was supported by grants from Citizens United for Research in Epilepsy (to E.G.), the National Institutes of Health (R01NS100954 and R01NS099188 to E.G.), and an Ike Muslow Predoctoral Fellowship (to H.D.) from Louisiana State University Health Sciences Center- Shreveport.

Conflicts of interests

The authors declare no competing financial interests.

References

Aiba, I., Noebels, J.L., 2015. Spreading depolarization in the brainstem mediates sudden cardiorespiratory arrest in mouse SUDEP models. Sci. Transl. Med. 7, 282ra46. https://doi.org/10.1126/scitranslmed.aaa4050.

Anderson, T.M., Ramirez, J.-M., 2017. Respiratory rhythm generation: triple oscillator hypothesis. F1000Research 6, 139. https://doi.org/10.12688/f1000research.10193.1.

Bird, J., Dembny, K., Sandeman, D., Butler, S., 1997. Sudden unexplained death in epilepsy: an intracranially monitored case. Epilepsia 38, S52–S56.

Dasheiff, R.M., Dickinson, L.J., 1986. Sudden unexpected death of epileptic patient due to cardiac arrhythmia after seizure. Arch. Neurol. 43, 194–196.

Devinsky, O., Hesdorffer, D.C., Thurman, D.J., Lhatoo, S., Richerson, G., 2016. Sudden unexpected death in epilepsy: epidemiology, mechanisms, and prevention. Lancet Neurol. 15, 1075–1088. https://doi.org/10.1016/S1474-4422(16)30158-2.

Dlouhy, B.J., Gehlbach, B.K., Kreple, C.J., Kawasaki, H., Oya, H., Buzza, C., Granner, M.A., Welsh, M.J., Howard, M.A., Wemmie, J.A., Richerson, G.B., 2015. Breathing inhibited when seizures spread to the amygdala and upon amygdala stimulation. J. Neurosci. 35, 10281–10289. https://doi.org/10.1523/JNEUROSCI.0888-15.2015.

Durand, E., Dauger, S., Pattyn, A., Gaultier, C., Goridis, C., Gallego, J., 2005. Sleep-disordered breathing in newborn mice heterozygous for the transcription factor Phox2b. Am. J. Respir. Crit. Care Med. 172, 238–243. https://doi.org/10.1164/rccm.200411-1528OC.

Gautier, N.M., Glasscock, E., 2015. Spontaneous seizures in Kcna1-null mice lacking voltage-gated Kv1.1 channels activate Fos expression in select limbic circuits. J. Neurochem. 135, 157–164. https://doi.org/10.1111/jnc.13206.

Glasscock, E., 2014. Genomic biomarkers of SUDEP in brain and heart. Epilepsy Behav. 38, 172–179. https://doi.org/10.1016/j.yebeh.2013.09.019.

Glasscock, E., Yoo, J.W., Chen, T.T., Klassen, T.L., Noebels, J.L., 2010. Kv1.1 potassium channel deficiency reveals brain-driven cardiac dysfunction as a candidate mechanism for sudden unexplained death in epilepsy. J. Neurosci. 30, 5167–5175. https://doi.org/10.1523/JNEUROSCI.5591-09.2010.

Glasscock, E., Qian, J., Kole, M.J., Noebels, J.L., 2012. Transcompartmental reversal of single fibre hyperexcitability in juxtaparanodal Kv1.1-deficient vagus nerve axons by activation of nodal KCNQ channels. J. Physiol. 590, 3913–3926. https://doi.org/10.1113/jphysiol.2012.235606.

Glasscock, E., Voigt, N., McCauley, M.D., Sun, Q., Li, N., Chiang, D.Y., Zhou, X.-B., Molina, C.E., Thomas, D., Schmidt, C., Skapura, D.G., Noebels, J.L., Dobrev, D., Wehrens, X.H.T., 2015. Expression and function of Kv1.1 potassium channels in human atria from patients with atrial fibrillation. Basic Res. Cardiol. 110, 505. https://doi.org/10.1007/s00395-015-0505-6.

Goldman, A.M., Glasscock, E., Yoo, J., Chen, T.T., Klassen, T.L., Noebels, J.L., 2009. Arrhythmia in heart and brain: KCNQ1 mutations link epilepsy and sudden unexplained death. Sci. Transl. Med. 1, 2ra6. https://doi.org/10.1126/scitranslmed.3000289.

Hajek, M.A., Buchanan, G.F., 2016. Influence of vigilance state on physiological consequences of seizures and seizure-induced death in mice. J. Neurophysiol. 115, 2286–2293. https://doi.org/10.1152/jn.00011.2016.

Holst, A.G., Winkel, B.G., Risgaard, B., Nielsen, J.B., Rasmussen, P.V., Haunsø, S., Sabers, A., Uldall, P., Tfelt-Hansen, J., 2013. Epilepsy and risk of death and sudden unexpected death in the young: a nationwide study. Epilepsia 54, 1613–1620. https://doi.org/10.1111/epi.12328.

Javaheri, S., 2010. Central sleep apnea. Clin. Chest Med. 31, 235–248. https://doi.org/10.1016/j.ccm.2010.02.013.

Kahn, A., Blum, D., Rebuffat, E., Sottiaux, M., Levitt, J., Bochner, A., Alexander, M., Grosswasser, J., Muller, M.F., 1988. Polysomnographic studies of infants who subsequently died of sudden infant death syndrome. Pediatrics 82, 721–727.

Kim, Y., Bravo, E., Thirnbeck, C.K., Smith-Mellecker, L.A., Kim, S.H., Gehlbach, B.K., Laux, L.C., Zhou, X., Nordli, D.R., Richerson, G.B., 2018. Severe peri-ictal respiratory dysfunction is common in Dravet syndrome. J. Clin. Invest. 128, 1141–1153. https://doi.org/10.1172/JCI94999.

Klassen, T.L., Bomben, V.C., Patel, A., Drabek, J., Chen, T.T., Gu, W., Zhang, F., Chapman, K., Lupski, J.R., Noebels, J.L., Goldman, A.M., 2014. High-resolution molecular genomic autopsy reveals complex sudden unexpected death in epilepsy risk profile. Epilepsia 55, e6–e12. https://doi.org/10.1111/epi.12489.

Kline, D.D., Buniel, M.C.F., Glazebrook, P., Peng, Y.-J., Ramirez-Navarro, A., Prabhakar, N.R., Kunze, D.L., 2005. Kv1.1 deletion augments the afferent hypoxic chemosensory pathway and respiration. J. Neurosci. 25, 3389–3399. https://doi.org/10.1523/JNEUROSCI.4556-04.2005.

Lauritzen, M., Dreier, J.P., Fabricius, M., Hartings, J.A., Graf, R., Strong, A.J., 2011. Clinical relevance of cortical spreading depression in neurological disorders: migraine, malignant stroke, subarachnoid and intracranial hemorrhage, and traumatic brain injury. J. Cereb. Blood Flow Metab. 31, 17–35. https://doi.org/10.1038/jcbfm.2010.191.

Loonen, I.C.M., Jansen, N.A., Cain, S.M., Schenke, M., Voskuyl, R.A., Yung, A.C., Bohnet, B., Kozlowski, P., Thijs, R.D., Ferrari, M.D., Snutch, T.P., van den Maagdenberg, A.M.J.M., Tolner, E.A., 2019. Brainstem spreading depolarization and cortical dynamics during fatal seizures in Cacna1a S218L mice. Brain 142, 412–425. https://doi.org/10.1093/brain/awy325.

Marcouiller, F., Boukari, R., Laouafa, S., Lavoie, R., Joseph, V., 2014. The nuclear progesterone receptor reduces post-sigh apneas during sleep and increases the ventilatory response to hypercapnia in adult female mice. PLoS ONE 9, e100421. https://doi.org/10.1371/journal.pone.0100421.

Mishra, V., Karumuri, B.K., Gautier, N.M., Liu, R., Hutson, T.N., Vanhoof-Villalba, S.L., Vlachos, I., Iasemidis, L., Glasscock, E., 2017. Scn2a deletion improves survival and brain-heart dynamics in the Kcna1-null mouse model of sudden unexpected death in epilepsy (SUDEP). Hum. Mol. Genet. 26, 2091–2103. https://doi.org/10.1093/hmg/ddx104.

Mishra, V., Gautier, N.M., Glasscock, E., 2018. Simultaneous video-EEG-ECG monitoring to identify Neurocardiac dysfunction in mouse models of epilepsy. J. Vis. Exp. JoVE. https://doi.org/10.3791/57300.

Moore, B.M., Jerry Jou, C., Tatalovic, M., Kaufman, E.S., Kline, D.D., Kunze, D.L., 2014. The Kv1.1 null mouse, a model of sudden unexpected death in epilepsy (SUDEP). Epilepsia 55, 1808–1816. https://doi.org/10.1111/epi.12793.

Nakamura, A., Kuwaki, T., 2003. Sleep apnea in mice: a useful animal model for study of SIDS? Early Hum. Dev. 75, S167–S174 Suppl.

Nakamura, A., Fukuda, Y., Kuwaki, T., 2003. Sleep apnea and effect of chemostimulation on breathing instability in mice. J. Appl. Physiol. 94, 525–532. https://doi.org/10.1152/japplphysiol.00226.2002.

Nakamura, A., Zhang, W., Yanagisawa, M., Fukuda, Y., Kuwaki, T., 2007. Vigilance state-dependent attenuation of hypercapnic chemoreflex and exaggerated sleep apnea in orexin knockout mice. J. Appl. Physiol. 102, 241–248. https://doi.org/10.1152/japplphysiol.00679.2006.

Nakase, K., Kollmar, R., Lazar, J., Arjomandi, H., Sundaram, K., Silverman, J., Orman, R., Weedon, J., Stefanov, D., Savoca, E., Tordjman, L., Stiles, K., Ihsan, M., Nunez, A., Guzman, L., Stewart, M., 2016. Laryngospasm, central and obstructive apnea during seizures: defining pathophysiology for sudden death in a rat model. Epilepsy Res. 128, 126–139. https://doi.org/10.1016/j.eplepsyres.2016.08.004.

Ramirez, J.-M., 2014. The integrative role of the sigh in psychology, physiology, pathology, and neurobiology. Prog. Brain Res. 209, 91–129. https://doi.org/10.1016/B978-0-444-63274-6.00006-0.

Real, C., Popa, D., Seif, I., Callebert, J., Launay, J.-M., Adrien, J., Escourrou, P., 2007. Sleep apneas are increased in mice lacking monoamine oxidase a. Sleep 30, 1295–1302.

Roundtree, H.M., Simeone, T.A., Johnson, C., Matthews, S.A., Samson, K.K., Simeone, K.A., 2016. Orexin receptor antagonism improves sleep and reduces seizures in Kcna1-null mice. Sleep 39, 357–368. https://doi.org/10.5665/sleep.5444.

Russell, A.E., 1906. Cessation of the pulse during the onset of epileptic fits,: with remarks on the mechanism of fits. Lancet 4325 (168), 152–154. https://doi.org/10.1016/S0140-6736(01)30477-4. Originally published as Volume 2.

Ryvlin, P., Nashef, L., Lhatoo, S.D., Bateman, L.M., Bird, J., Bleasel, A., Boon, P., Crespel, A., Dworetzky, B.A., Høgenhaven, H., Lerche, H., Maillard, L., Malter, M.P., Marchal, C., Murthy, J.M.K., Nitsche, M., Pataraia, E., Rabben, T., Rheims, S., Sadzot, B., Schulze-Bonhage, A., Seyal, M., So, E.L., Spitz, M., Szucs, A., Tan, M., Tao, J.X., Tomson, T., 2013. Incidence and mechanisms of cardiorespiratory arrests in epilepsy monitoring units (MORTEMUS): a retrospective study. Lancet Neurol. 12, 966–977. https://doi.org/10.1016/S1474-4422(13)70214-X.

Sheikhbahaei, S., Gourine, A.V., Smith, J.C., 2017. Respiratory rhythm irregularity after carotid body denervation in rats. Respir. Physiol. Neurobiol. 246, 92–97. https://doi.org/10.1016/j.resp.2017.08.001.

Shorvon, S., Tomson, T., 2011. Sudden unexpected death in epilepsy. Lancet 378, 2028–2038. https://doi.org/10.1016/S0140-6736(11)60176-1.

Si, M., Trosclair, K., Hamilton, K.A., Glasscock, E., 2018. Genetic ablation or pharmacological inhibition of Kv1.1 potassium channel subunits impairs atrial repolarization in mice. Am. J. Phys. Cell Phys. 316, C154–C161. https://doi.org/10.1152/ajpcell.00335.2018.

Simeone, K.A., Hallgren, J., Bockman, C.S., Aggarwal, A., Kansal, V., Netzel, L., Iyer, S.H., Matthews, S.A., Deodhar, M., Oldenburg, P.J., Abel, P.W., Simeone, T.A., 2018. Respiratory dysfunction progresses with age in Kcna1-null mice, a model of sudden unexpected death in epilepsy. Epilepsia 59, 345–357. https://doi.org/10.1111/epi.13971.

Smart, S.L., Lopantsev, V., Zhang, C.L., Robbins, C.A., Wang, H., Chiu, S.Y., Schwartzkroin, P.A., Messing, A., Tempel, B.L., 1998. Deletion of the K(V)1.1 potassium channel causes epilepsy in mice. Neuron 20, 809–819.

Stettner, G.M., Huppke, P., Brendel, C., Richter, D.W., Gärtner, J., Dutschmann, M., 2007. Breathing dysfunctions associated with impaired control of postinspiratory activity in Mecp2−/y knockout mice. J. Physiol. 579, 863–876. https://doi.org/10.1113/jphysiol.2006.119966.

Thurman, D.J., Hesdorffer, D.C., French, J.A., 2014. Sudden unexpected death in epilepsy: assessing the public health burden. Epilepsia 55, 1479–1485. https://doi.org/10.1111/epi.12666.

Yamauchi, M., Ocak, H., Dostal, J., Jacono, F.J., Loparo, K.A., Strohl, K.P., 2008. Post-sigh breathing behavior and spontaneous pauses in the C57BL/6J (B6) mouse. Respir. Physiol. Neurobiol. 162, 117–125. https://doi.org/10.1016/j.resp.2008.05.003.

Zuberi, S.M., Eunson, L.H., Spauschus, A., De Silva, R., Tolmie, J., Wood, N.W., McWilliam, R.C., Stephenson, J.B., Stephenson, J.P., Kullmann, D.M., Hanna, M.G., 1999. A novel mutation in the human voltage-gated potassium channel gene (Kv1.1) associates with episodic ataxia type 1 and sometimes with partial epilepsy. Brain 122, 817–825 Pt 5.